Concentration- and Solvent-Dependent Excimer Formation of 1-Pyrenylmethanamine, Covalently Attached to Maleic Anhydride-Grafted Ethylene–Propylene Copolymers

Sándor Németh,[1] Tze-Chi Jao,[2] and Janos H. Fendler*,[1]

Department of Chemistry, Syracuse University, Syracuse, New York 13244-4100, and Texaco R&D Department, P.O. Box 509, Beacon, New York 12508

Received February 4, 1994; Revised Manuscript Received June 23, 1994®

ABSTRACT: The association behavior of a maleic anhydride-grafted ethylene–propylene copolymer, EP(60/40), has been studied by several methods in hexane and tetrahydrofuran (THF). The concentration-dependent apparent hydrodynamic diameters ($\bar{D}_H$) of EP(60/40) have been determined at 25.0 °C by dynamic light scattering. $\bar{D}_H$ have been found to increase exponentially in both solvents. However, in THF $\bar{D}_H$ are much smaller and their increase with increasing concentrations of EP(60/40) is less steep than that in hexane. A pyrene-labeled ($\bar{M}_W$ = 40 000) EP(60/40), P-EP(60/40), has been prepared. Absorption, excitation, and emission spectroscopic measurements have provided evidence for the presence of ground-state pyrene complexes of P-EP(60/40) in hexane. In contrast, no evidence has been found for ground-state complex formation in THF by using these criteria. Treatment of the concentration-dependent excimer-to-monomer ratios has permitted the assessment of the equilibrium constants, aggregation numbers, and Gibbs free energy for the association of P-EP(60/40).

Introduction

The beneficial properties of ethylene–propylene and related copolymers have prompted their increasing use as motor oil additives.[3] Ethylene–propylene copolymers have been found to be useful as viscosity modifiers; they enhanced the viscosities of hydrocarbon solvents to a greater extent at high, than at low, temperatures.[4] This property has been suggested to be related to the complex composition, temperature- and solvent-dependent association, and conformation changes of the copolymer.[5] The experimental approach for the verification of this suggestion included intrinsic viscosity, light scattering, and fluorescence measurements.[5-7] Absorption, excitation, and emission spectra and nanosecond fluorescence lifetime measurements of a pyrene-labeled, functionalized, $\bar{M}_W$ = 1.48×10^5 ethylene–propylene copolymer have provided evidence, for example, for the formation of ground-state complexes in methylcyclohexane, but not in tetrahydrofuran.[8]

In spite of the importance of lower-molecular-weight copolymers as dispersants,[9] no detailed information is available on their solution behavior. We have, therefore, launched investigations into the concentration- and solvent-dependent conformational changes of $\bar{M}_W$ = 4.0×10^4 ethylene–propylene copolymers which contained 60 mol % ethylene and 40 mol % propylene and which were grafted with maleic anhydride, EP(60/40). Concentration-dependent excimer formation of 1-pyrenylmethanamine (PMA)-labeled, low-molecular-weight EP(60/40), P-EP(60/40), is reported in the present publication. Advantage has been taken of the recently determined excimer formation behavior of the model compound, 1-pyrenylmethanamine,[10] in inferring ground-state pyrene complex formation, as well as intra- and intermolecular associations of low-molecular-weight EP(60/40) in hexane and tetrahydrofuran (THF). The label (PMA) was chosen since it has a short side chain ($-CH_2NH_2$) and is quite rigidly attached to the polymer backbone through the succinic anhydride groups (Scheme 1). The probe reports, therefore, the coiling of the polymer without the interference of a flexible bridge between the polymer and the pyrene group. In addition to the measurements of absorption, excitation, and emission spectra and fluorescence decay profiles, we have also determined the apparent hydrodynamic radii and molecular weights of this copolymer by dynamic and static light scattering in hexane and THF, as well as the equilibrium constants and aggregation numbers for P-EP(60/40) association.

Scheme 1

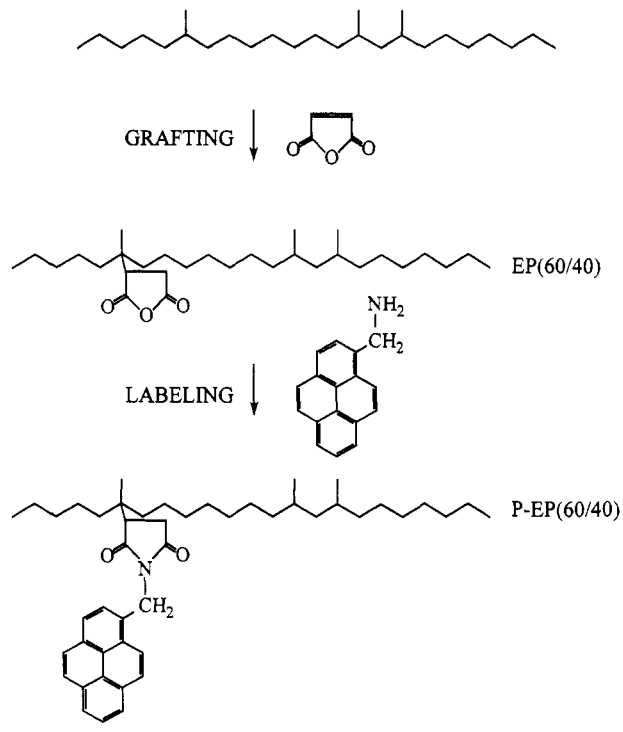

Experimental Section

Ethylene–propylene copolymer, EP(60/40), grafted by maleic anhydride (2%, w/w) with a number-averaged molecular weight of $\bar{M}_N$ = 14 000, was used as received from Texaco, Inc. Ammonium hydroxide, toluene, and acetone (Fisher; certified ACS grade) were used as received. Hexane (American Scientific Products; UV grade) and THF (Aldrich; HPLC grade) were purified by distillation.

® Abstract published in *Advance ACS Abstracts*, August 1, 1994.

0024-9297/94/2227-5449$04.50/0

The preparation, purification, and characterization of the fluorescence label, 1-pyrenylmethanamine hydrochloride, have been described.[10] Fluorescence-labeled EP copolymer, P-EP(60/40), was prepared as follows. 1-Pyrenylmethanamine hydrochloride [0.1222 g (0.456 mmol)] was transferred into a separatory funnel along with 40 mL of toluene and 15 mL of concentrated ammonium hydroxide. The water phase was removed, and the organic layer was washed twice with water (20 mL), collected, and dried by distilling out the water–toluene azeotrope. The obtained amine solution (1.13×10^{-4} mol in 25 mL of toluene) was added dropwise to a stirred toluene (10 mL) solution of EP(60/40) (0.39 g). The reaction mixture was refluxed for 1 h. The produced water was distilled out as a water–toluene azeotrope. The reaction mixture was cooled down, and the labeled polymer was precipitated by the addition of acetone. The precipitated P-EP(60/40) was dissolved in toluene again, reprecipitated by acetone, and dried. The attachment of the label was characterized by gel permeation chromatography (GPC; Perkin-Elmer Series 400 liquid chromatograph equipped with a Perkin-Elmer LC95 UV–visible spectrophotometer detector set to 344 nm; 10^3- and 10^4-Å 7.8 × 300 mm Waters Ultrastyragel columns in series, eluted with THF at 23 °C). Absorption spectra were taken on a Hewlett-Packard 8450 diode array spectrophotometer. The label content was determined by absorption spectrophotometry. Extinction coefficients of the pyrene label in the polymer ($\epsilon_{314\ nm}$ = 1.26 L g^{-1} cm^{-1}, $\epsilon_{327\ nm}$ = 2.93 L g^{-1} cm^{-1}, $\epsilon_{344\ nm}$ = 4.4 L g^{-1} cm^{-1}) were assumed to be identical to those in THF ($\epsilon_{314\ nm}$ = 11 900 M^{-1} cm^{-1}, $\epsilon_{327\ nm}$ = 27 400 M^{-1} cm^{-1}, $\epsilon_{344\ nm}$ = 39 800 M^{-1} cm^{-1}). Using these extinction coefficients led to a label content of (1.05 ± 0.03) × 10^{-4} mol of pyrene per 1.0 g of polymer. Taking the number-averaged molecular weight, $\bar{M}_N$, of the polymer to be 1.4×10^4 leads, on the average, to 1.5 labels per molecule.

Excitation and emission spectra were taken on a Spex fluorolog instrument equipped with a Tracor Northern TN 6500 rapid scan spectrometer detection system. Steady-state fluorescence measurements were performed in hexane and THF solutions of P-EP(60/40) samples, deoxygenated on the high-vacuum line by repeated (at least five times) freeze–pump–thaw cycles.

Excitation spectra were obtained by measuring the intensity of the fluorescence light (I_F) at a certain wavelength while varying the excitation wavelength. The excitation light was split by a quartz plate, and part of it was directed to a quantum counter and monitored (I_i). The quantum counter consisted of an ethylene glycol solution of 3 g/L of rhodamine B in a 0.5-cm quartz cell. Light passing through the quantum counter was measured by a (Hamamatsu R508) PM tube whose output signal was observed by an electrometer. After correction for dark current, the electrometer output was proportional to I_i.

Since I_F is proportional to $I_0 A_s$ at low optical densities, where A_s is the absorbance due to the solute and I_0 is the intensity of the exciting light in the observed volume element, the excitation spectra can be calculated from $I_0 = I_i$ at low absorbances (0.01/cm or less) or from:

$$I_0 = I_i \times 10^{-AL} \tag{1}$$

where L is the path length of the excitation light between the wall of the cell and the volume element under observation and A is the total absorbance of the solution. Using N as the normalization factor, the corrected excitation spectrum as a function of wavelength, $S(\lambda)$, was calculated from:

$$S(\lambda) = N I_F(\lambda)/I_0(\lambda) \tag{2}$$

Dynamic light scattering measurements were performed by a Model PR 102 spectrometer system (Malvern Instruments). The signal of the PM tube of the instrument was analyzed by a Model BI-2030AT digital correlator with 72 data channels and an attached IBM-AT computer (Brookhaven). A Spectra Physics 2020 argon ion laser (514.5 nm) was used as the light source. The apparent average diffusion coefficients were determined by the cumulant technique at a 90° scattering angle.[11] The corresponding apparent hydrodynamic diameters were calculated by the Stokes–Einstein equation. The viscosity of hexane was taken to be 0.295 cP at 25.0 °C and 0.214 cP at 60.0 °C,[12] and the viscosity of THF was taken to be 0.460 cP at 25.0 °C.[13] Dust particles were removed from stock solutions by centrifugation (at 7000 rpm) for 10 min. The supernatant was collected and used for the preparation of samples diluted with carefully cleaned (distilled in a dust-free nitrogen atmosphere) solvent. These diluted samples were sealed into Pyrex tubes for light scattering.

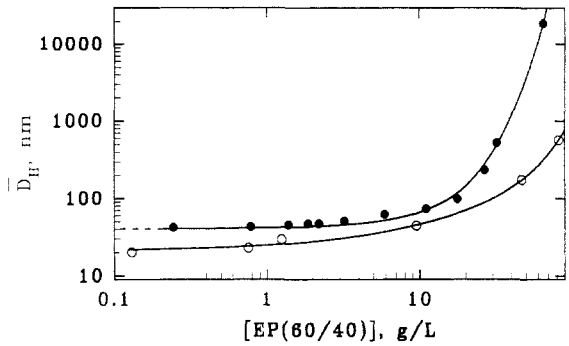

Figure 1. Dependence of the apparent hydrodynamic diameter, $\bar{D}_H$, on EP(60/40) concentration in hexane (●) and in THF (○) at 25.0 °C (double-logarithmic plot). Solid lines are results of the fittings described in the text.

Results and Discussion

1. Concentration- and Solvent-Dependent Size Changes. Treatment of Dynamic Light Scattering Data. The dynamic light scattering experiments indicated a very steep and significant increase in the apparent hydrodynamic diameter ($\bar{D}_H$) of the polymer with increasing concentrations (c) of EP(60/40) in hexane (Figure 1), which can be adequately described by an exponential curve of three parameters [$\bar{D}_H = a_1 \exp(a_2 c) + a_3$]. Extrapolating this curve to c = 0 g/L gave a limiting $\bar{D}_H$ value of 40 ± 2 nm (corresponding to an apparent average diffusion coefficient of (3.7 ± 0.2) × 10^{-7} cm^2 s^{-1}). The $\bar{D}_H$ allowed the estimation of the lower limit of the upper concentration at which polymer coils do not overlap to be 0.5 g/L.[14] The temperature dependence of $\bar{D}_H$ in hexane was measured for a sample at a concentration of 0.24 g/L. The diameter was found to decrease from 42.3 ± 0.1 nm at 25 °C to 39.2 ± 1.0 nm at 60 °C, less than 10%.

The concentration dependence of $\bar{D}_H$ in tetrahydrofuran is significantly less pronounced. The $\bar{D}_H$ of EP(60/40) is much lower and the increase is less steep with increasing concentrations. The experimental points can be fitted by a modified exponential curve [$\bar{D}_H = a'_1 \exp(a'_2 c) + a'_3 c^{0.7}$] which yields a limiting $\bar{D}_H$ value of 21 nm upon extrapolating to c = 0 g/L (Figure 1). Dynamic light scattering parameters for EP(60/40) are collected in Table 1.

The most important results from the dynamic light scattering measurements are the relatively small changes of $\bar{D}_H$ in the lower concentration range (0.2–1.0 g/L), indicating negligible changes in the size of the polymer coils in both solvents and in the considerably larger diameters and corresponding volumes in hexane than in THF. These results indicate a considerably stronger interaction between the polymer molecules in hexane than in THF and imply a possible association process of EP(60/40) in the former solvent.

2. Solvent-Dependent Weight-Averaged Molecular Weights. Treatment of Steady-State Light Scattering Determinations. The weight-averaged molecular weight of EP(60/40) ($\bar{M}_W$) was determined in hexane and in THF by measurements of the intensities of scattered light at different scattering angles and polymer concentrations. The basic equation of this measurement is[15]

Table 1. Dynamic Light Scattering of P-EP(60/40) in Hexane and THF[a]

	$\bar{D}_H$, nm		Q^b	
[P-EP(60/40)], g/L	hexane	THF	hexane	THF
82.0		571.0		0.310
65.0	19000			
47.6		175.0		0.380
32.2	528.3		0.363	
26.7	235.3		0.342	
17.6	99.1		0.333	
11.0	73.6		0.296	
9.5		44.0		0.340
5.90	62.1		0.286	
3.21	50.9		0.258	
2.20	47.2		0.245	
1.86	47.2		0.247	
1.39	45.9		0.248	
1.25		29.5		0.490
0.785	43.2		0.238	
0.753		22.8		0.450
0.243	42.3		0.25	
0.130		20.0		0.610

[a] Temperature: 25.0 °C; 90° scattering angle. [b] Polydispersity, the square of the relative standard deviation of the diameter distribution.

$$M^* = \nu^{-2}[\nu_A\nu_B\bar{M}_W + W\bar{M}_W{}^A(\nu_A{}^2 - \nu_A\nu_B) + (1 - W)\bar{M}_W{}^B(\nu_B{}^2 - \nu_A\nu_B)] \quad (3)$$

where M^* is the apparent molecular weight (depending on the solvent due to the different refractive index increments of the A and B constituents of the copolymer); ν, ν_A, and ν_B are the refractive index increments of the copolymer, homopolymer A, and homopolymer B, respectively (A = polyethylene, B = polypropylene); $\bar{M}_W$ is the weight-averaged molecular weight of the copolymer; W is the weight fraction of constituent A; and $\bar{M}_W{}^A$ and $\bar{M}_W{}^B$ are the weight-averaged partial molecular weights of the copolymer due to A and B, respectively. Furthermore

$$\nu = W\nu_A + (1 - W)\nu_B \quad (4)$$

The refractive index increments in hexane and THF of EP(60/40) were determined, by means of an Abbe refractometer (using Na D line, 25 °C), to be 0.124 and 0.087 mL/g. The value in hexane agreed well with that reported for polypropylene (0.1152 mL/g).[16] This fact ($\nu = \nu_A = \nu_B$) greatly simplifies eq 3 ($M^* = \bar{M}_W$) and permits the application of the usual formalism of light scattering.[17]

$$\frac{K^*c}{\Delta R} = \frac{1}{\bar{M}_W P(\theta)} + 2A_2c + \ldots \quad (5)$$

where ΔR is the difference of the Rayleigh ratio of the soltuion and pure solvent; $P(\theta)$ is the scattering function (approaching 1 when θ, the scattering angle, tends to 0); A_2 is the second virial coefficient; and c is the concentration. K^* is defined, for optically polarized incident light, by:

$$K^* = 4\pi^2 n_0{}^2 \nu^2 / N_A \lambda_0{}^4 \quad (6)$$

where n_0 is the refractive index of the solvent; N_A is Avogadro's number; and λ_0 is the wavelength of the light in vacuum. Using eq 5 and extrapolating to $\theta = 0$ and $c = 0$ yielded $\bar{M}_W = (9.1 \pm 0.9) \times 10^5$ in hexane and $\bar{M}_W = (4.0 \pm 0.4) \times 10^4$ in THF, giving a weight-averaged aggregation number of 23. The Zimm plot in hexane is illustrated in Figure 2.

3. Ground-State Association. Treatment of Absorption, Excitation, and Emission Spectra. The absorption spectrum of P-EP(60/40) in hexane (Figure 3)

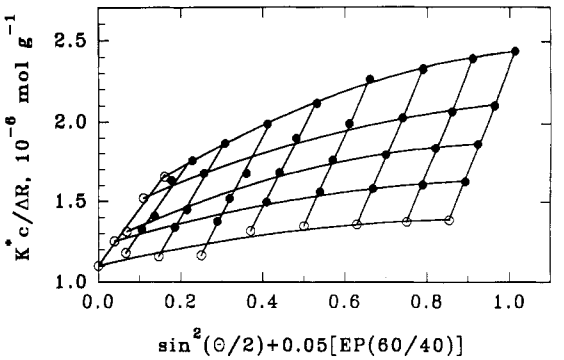

Figure 2. Zimm plot of EP(60/40) in hexane measured at eight angles (from 30° to 135° by 15° increments) and four concentrations (3.21, 2.20, 1.39, and 0.705 g/L) at 25 °C. Solid circles represent the measured points, and empty circles represent the extrapolated ones.

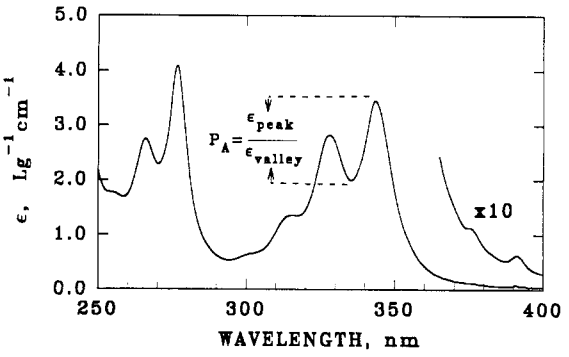

Figure 3. Decadic extinction coefficients (ϵ in L g^{-1} cm^{-1}) of P-EP(60/40) in hexane as a function of wavelength at ambient temperature. The ratio of the absorption intensity of the most intense band of the $S_0 \rightarrow S_2$ transition to that of the adjacent minimum at the shorter wavelength is defined as P_A.

Table 2. Spectroscopic Parameters Measured in Organic Solutions of 1-Pyrenylmethanamine (PMA) and P-EP(60/40)[a]

	PMA[b]		P-EP(60/40)	
	hexane	THF	hexane	THF
P_A	3.1	2.6	1.7	2.7
P_M	2.7	2.2	2.1	2.3
P_E	(2.7)	(2.2)	1.7	2.1
$\Delta\lambda$, nm	(0)	(0)	1.3	<0.5[c]

[a] See Results and Discussion section and Figures 3 and 5 for definitions. Determined at ambient temperatures at PMA concentrations of 5.0×10^{-7} M and of P-EP(60/40) concentrations of 0.11 (in hexane) and 0.038 g/L (in THF). [b] Taken from ref 10. Values in parentheses cannot be measured accurately since excimer formation occurs only at relatively high concentrations where the excitation spectrum is distorted due to excess absorption. [c] Within the limit of resolution.

is characterized by bands with maxima at 277 (ϵ = 4.13 L g^{-1} cm^{-1}), 315 (ϵ = 1.36 L g^{-1} cm^{-1}), 328 (ϵ = 2.85 L g^{-1} cm^{-1}), and 344 nm (ϵ = 3.44 L g^{-1} cm^{-1}). This spectrum is considerably different from that of 1-pyrenylmethanamine in the same solvent.[10] The absorption maxima of P-EP(60/40) shifted 2–3 nm to lower wavelengths from those in 1-pyrenylmethanamine. The ratio of the absorption intensity of the most intense band above 300 nm to that of the adjacent minimum at the shorter wavelength, P_A (see Figure 3), has been found to be 1.7 for the copolymer in hexane, on contrast to 2.7 in THF. These values, in comparison with those obtained for the free label (see values for PMA in Table 2), indicate appreciable ground-state pyrene association of P-EP(60/40) in hexane, but not in THF.[18]

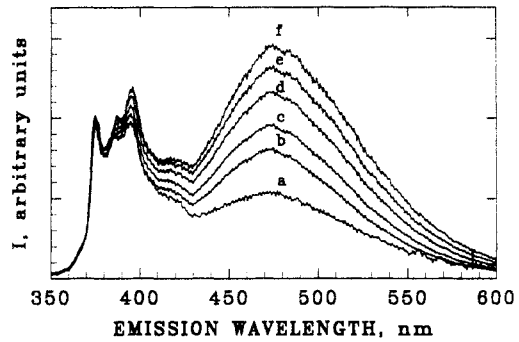

Figure 4. Plot of corrected emission spectra for 0.0038 (a), 0.020 (b), 0.76 (c), 1.47 (d), 2.42 (e), and 3.80 (f) g/L P-EP(60/40) is deoxygenerated (five freeze–thaw–pump cycles on a high-vacuum line) hexane solutions. Each spectrum was normalized to the peak of the monomer emission at 374 nm. λ_{ex} = 310 nm, front-face illumination. Bandwidth: 4-nm excitation, 25-nm emission (20 °C).

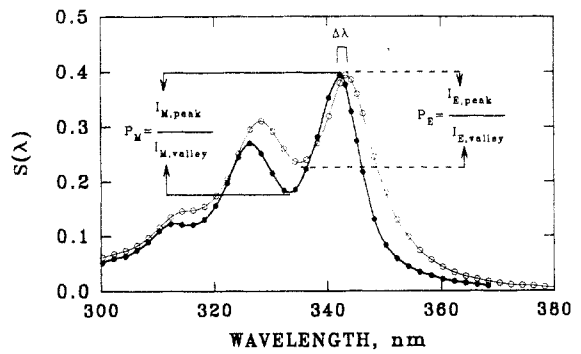

Figure 5. Excitation spectra of 0.11 g/L of P-EP(60/40), viewed at the monomer (●) and excimer (○) emissions. Values of P_M, P_E, and $\Delta\lambda$ are defined. S(λ) is described in the text.

Excitation of a 3.8 × 10^{-3} g/L solution of P-EP(60/40) in hexane resulted in the appearance of a fluorescence with emission maxima at 374 and 474 nm (see a in Figure 4). Increasing the concentration of P-EP(60/40) from 3.8 × 10^{-3} to 3.8 g/L in hexane progressively increased the intensity of the longer wavelength emission band (see a → f in Figure 4). This behavior is characteristic, of course, for the formation of the [P-EP(60/40)–P-EP(60/40)]* excimer.

Ground-state association of P-EP(60/40) in hexane is also evidenced in the absence of overlap of the absorption and excitation spectra, as well as in the difference between the excitation spectra if followed at the monomer and excimer emissions, in both shape and position (Figure 5), indicating the presence of more than one fluorescence species. The peak-to-valley ratio for the (0,0) transition in the excitation spectrum viewed at the monomer emission, P_M, and at the excimer emission, P_E, is also shown in Figure 5. Peak-to-valley ratios in the absorption and emission spectra, as well as the shift in the wavelength maxima of the (0,0) transition in the two excitation spectra, $\Delta\lambda = \lambda_{max}$(excimer) − λ_{max}(monomer), for PMA in hexane and in THF and for P-EP(60/40) in hexane and THF are collected in Table 2. The contrasting behavior of P-EP(60/40) in the two solvents is evident. Ground-state complexation in THF is negligible, but it is substantial in hexane, as is shown by exploiting the differences in the spectroscopic properties of the free and preassociated chromophores.

4. Ground-State Association. Treatment of Concentration- and Solvent-Dependent Excimer Formation Data. The two emission bands of P-EP(60/40) with maxima at 374 and 474 nm in hexane solutions (Figure 4)

Table 3. Excimer–Monomer Intensity Ratios of P-EP(60/40) in Hexane[a]

[P-EP(60/40)], g/L	I_E/I_M[b]	[P-EP(60/40)], g/L	I_E/I_M[b]
3.80	3.24	0.029	1.45
2.42	2.88	0.0145	1.40
1.47	2.46	0.0089	1.34
0.76	1.99	0.0062	1.28
0.310	1.73	0.0038	1.17
0.200	1.69	0.0030	1.14
0.093	1.58	0.0022	1.08
0.069	1.56	0.0018	1.02
0.052	1.54	0.0011	0.87
0.038	1.50		

[a] Degassed samples by five freeze–pump–thaw cycles (1 × 10^{-5} Torr). λ_{ex} = 310 nm. [b] I_E/I_M was calculated by dividing the total intensity of the excimer band by the total intensity of the monomer band using corrected spectra, determined at 20.0 °C.

Table 4. Excimer–Monomer Intensity Ratios of P-EP(60/40) in THF[a]

[P-EP(60/40)], g/L	I_E/I_M[b]	[P-EP(60/40)], g/L	I_E/I_M[b]
0.236	1.51	0.0210	1.49
0.179	1.51	0.0130	1.47
0.140	1.51	0.0029	1.44
0.111	1.51	0.0020	1.45
0.0776	1.50	0.0006	1.44
0.0541	1.49	0.0004	1.42
0.0353	1.49		

[a] Degassed samples by five freeze–pump–thaw cycles (1 × 10^{-5} Torr). λ_{ex} = 310 nm. [b] I_E/I_M was calculated by dividing the total intensity of the excimer band by the total intensity of the monomer band using corrected spectra, determined at 20.0 °C.

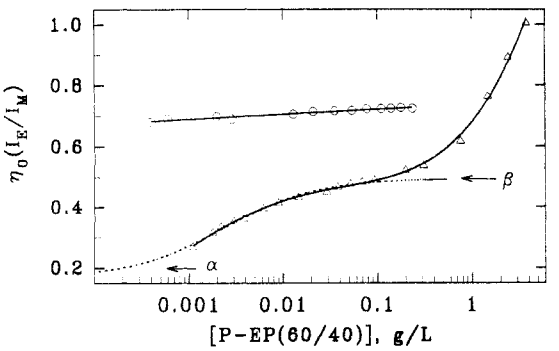

Figure 6. Plot of the excimer–monomer ratio corrected by solvent viscosity (η_0) *vs* [P-EP(60/40)] in hexane (Δ) and in THF (○) (20 °C; front-face illumination). The broken line represents the fitted curve resulting in K_0 = 1.3 × 10^7 L mol^{-1}. See the Results and Discussion section for the meaning of α and β.

can be assigned to monomer and excimer emissions. Excimer–monomer ratios of P-EP(60/40) in hexane and THF at different concentrations are collected in Tables 3 and 4 and are plotted at 20.0 °C in Figure 6. The distribution of the fluorescence label is statistical (there are 1.5 labels per polymer on the mean); excimers can form both intermolecularly and intramolecularly if the concentration of P-EP(60/40) is sufficiently high. Intramolecular excimer formation is the consequence of coiling of the polymer chains having at least two labels on them.[19] Alternatively, it can be due to preassociated pyrenes excited directly into the excimer state. Since $\eta_0(I_E/I_M)$ is higher for THF solutions in the low concentration range, it is obvious (with the assumption of similar quantum efficiencies of the pyrene moieties in both solvents) that hexane is a better solvent for P-EP(60/40). Excimer formation is known to be less favorable in expanded polymer coils.[20] The solubility parameters also indicate this. They are δ = 7.3 for hexane,[13] δ = 9.9 for THF,[13] and δ = 7.7 for an EP copolymer.[21] In spite of the fact that

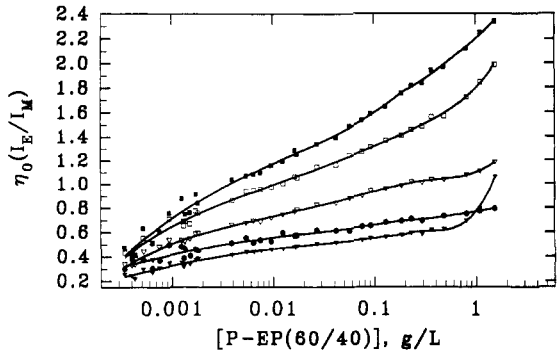

Figure 7. Excimer-to-monomer ratios corrected by solvent viscosity (η_0) *vs* P-EP(60/40) concentration at different excitation wavelengths (▼, 340 nm; ●, 310 nm; ▽, 332 nm; □, 348 nm; ■, 350 nm) in hexane (25.0 °C, right-angle illumination).

THF is not as good of a solvent as hexane, no ground-state complexation was observed in the former solvent, indicating the significance of solvent polarity and, thus, the importance of succinimide polar groups in ground-state complex formation, as well as in the association process. This result qualitatively suggests that the driving force of association is dipole–dipole interaction of the succinimide groups.

Covalent attachment of the fluorescence probe to the polymer backbone was demonstrated by GPC. The presence of excimer emission, even at a P-EP(60/40) concentration as low as 1.1×10^{-3} g/L, is in accord with the covalent link of a pyrene moiety to the P-EP(60/40). *A priori*, one would expect the excimer-to-monomer ratio to be concentration independent for intramolecular excimers at sufficiently low P-EP(60/40) concentrations. This was indeed found to be the case in THF at the P-EP(60/40) concentration range of 0.001–0.3 g/L. In hexane, however, there was a continuous decrease of the excimer-to-monomer ratio with decreasing P-EP(60/40) concentration (in the entire 0.001–3.8 g of P-EP(60/40)/L concentration range; Figure 6). This behavior is explicable in terms of concentration-dependent ground-state association of P-EP(60/40). Dilution results in the dissociation of ground-state complexes which increases the monomeric pyrene concentration and, hence, decreases the excimer–monomer ratio. A similar behavior has been reported for excimer formation in hydroxypropylcellulose solutions randomly labeled by pyrene.[22]

The fluorescence from P-EP(60/40) was followed as a function of excitation wavelength and polymer concentration in hexane (25 °C, right-angle arrangement). The obtained curves are shown in Figure 7. It is obvious that there is a contribution to the excimer–monomer ratio due to the excitation of the preassociated pyrenes, even at the lowest available concentration, since the curves do not reach each other. However, it appears that the ground-state contribution to the excimer–monomer ratios increases with increasing polymer concentrations. This can be deduced from the different shape of the curves depending on the excitation wavelength. The slopes are the least steep for the 310- and 340-nm excitations, while they are the steepest for the 348- and 350-nm excitations. The former wavelengths more efficiently excite the pyrenes not involved in ground-state complexes, while the latter ones are more specific for the ground-state complexes. This indicates a higher contribution to the excimer-to-monomer ratios from the excitation of the ground-state pyrene complexes as the concentration increases.

5. Equilibrium Constants for P-EP(60/40) Association and Aggregation Numbers. Treatment of Concentration-Dependent Excimer Formation Data. Polymer aggregation can be followed via the concentration dependence of the excimer-to-monomer ratio. The relationship between the equilibrium constant for the association of P-EP(60/40) and the excimer-to-monomer ratio can be estimated by making some assumptions. Specifically, treating the polymer as if it was a monodisperse system of identical associating molecules and assuming identical equilibrium constants of association (K_0) for each step leads to eqs 7 and 8.

$$\text{P-EP}_1 + \text{P-EP}_1 \rightleftharpoons \text{P-EP}_2 \tag{7}$$

$$K_0 = [\text{P-EP}_2]/[\text{P-EP}_1]^2 \tag{8}$$

Further steps of (open) multimerization can be given similarly:[23]

$$k\text{P-EP}_1 \rightleftharpoons \text{P-EP}_k \tag{9}$$

$$K_0^{k-1} = \frac{[\text{P-EP}_k]}{[\text{P-EP}_1]^k} \tag{10}$$

From eq 10, one can calculate the concentration of the multimers made up of k P-EP(60/40) molecules:

$$[\text{P-EP}_k] = K_0^{k-1}[\text{P-EP}_1]^k \tag{11}$$

where $[\text{P-EP}_1]$ is given by:[24]

$$[\text{P-EP}_1] = \frac{2K_0c + 1 - (4K_0c + 1)^{1/2}}{2K_0^2c} \tag{12}$$

where c is the total concentration of the polymer in mol/L units.

The excimer-to-monomer ratio increases upon association since the relative concentration of the ground-state pyrene complexes increases and, possibly, the dynamic excimer formation also becomes more favorable. This latter behavior could be explained by the increase of the number of pyrene molecules in the volume which is "scanned" by an excited pyrene during its lifetime. Qualitatively, the pyrene molecules attached to a polymer chain undergo Brownian motion and, due to this motion, they can "map" a certain volume element during the lifetime of the excited pyrene. Upon the addition of further labeled molecules through association, the number of pyrenes is increased within the volume element experienced by the excited pyrene. This can lead to more favorable formation of excimers. After a certain stage of association, the increase in the number of pyrenes is confined to volume elements not reached by the excited pyrene chosen before and the increase in the excimer-to-monomer ratio vanishes. One can therefore expect a certain excimer-to-monomer ratio (call it α) for the polymer in the extremely dilute state when only individual coils and very small aggregates exist (not reached by experiments). After a certain extent of aggregation, the excimer-to-monomer ratio reaches its maximum value (call it β). The proposed α and β values are indicated in Figure 6.

Another assumption needs to be made at this point, namely, that α is the excimer-to-monomer ratio of associated multimers containing less than n molecules and β is produced if the number of molecules is at least n. The essence of this assumption is that the association can be followed as a one-step process with regard to the excimer-to-monomer ratio. The measured excimer-to-monomer ratio can be given as an average of α and β. For this, eqs 13–16 must be solved:

$$\alpha = I_E^{\alpha}/I_M^{\alpha} \qquad \beta = I_E^{\beta}/I_M^{\beta} \tag{13}$$

$$I_E = \sum_{i=1}^{n-1} i[\text{P-EP}_i]I_E^{\alpha} + \sum_{j=n}^{\infty} j[\text{P-EP}_j]I_E^{\beta} \tag{14}$$

$$I_M = \sum_{i=1}^{n-1} i[\text{P-EP}_i]I_M^{\alpha} + \sum_{j=n}^{\infty} j[\text{P-EP}_j]I_M^{\beta} \tag{15}$$

$$R = I_E/I_M \tag{16}$$

where subscripts E and M refer to the excimer and monomer, respectively, and R is the experimentally observed excimer to monomer ratio. Further equations can be set up by taking into account the relationship between the excimer and monomer emissions through the quantum efficiencies. If Φ_E and Φ_M are the quantum yields and q_E and q_M are the quantum efficiencies, then the following equation holds:[25]

$$\Phi_E/q_E + \Phi_M/q_M = 1 \tag{17}$$

Since I_E and I_M are proportional to Φ_E and Φ_M, respectively, eq 17 can be rewritten as:

$$I_E/q_E + I_M/q_M = \text{constant} \tag{18}$$

Equation 18 is true for any I_E and I_M in the same solvent, independent of concentration in the low and medium absorbance range, and can be used to establish relationships among the various fluorescence intensities above:

$$I_E^{\alpha}/q_E + I_M^{\alpha}/q_M = I_E^{\beta}/q_E + I_M^{\beta}/q_M \tag{19}$$

Choosing units of fluorescence intensity such that $I_M^{\alpha} = 1$ decreases the number of unknowns by 1. In this way, one can combine the above equations to obtain a smaller set with fewer variables. Using eq 13 allows the elimination of I_E^{α} and I_E^{β} from eqs 14 and 15:

$$I_E = \sum_{i=1}^{n-1} i[\text{P-EP}_i]\alpha + \sum_{j=n}^{\infty} j[\text{P-EP}_j]\beta I_M^{\beta} \tag{20}$$

$$I_M = \sum_{i=1}^{n-1} i[\text{P-EP}_i] + \sum_{j=n}^{\infty} j[\text{P-EP}_j]I_M^{\beta} \tag{21}$$

Equations 20 and 21 can be combined through eq 16 to give

$$R = \frac{\sum_{i=1}^{n-1} i[\text{P-EP}_i]\alpha + \sum_{j=n}^{\infty} j[\text{P-EP}_j]\beta I_M^{\beta}}{\sum_{i=1}^{n-1} i[\text{P-EP}_i] + \sum_{j=n}^{\infty} j[\text{P-EP}_j]I_M^{\beta}} \tag{22}$$

Furthermore, using eq 19 gives an expression for I_M^{β} (after substitution from eq 13 and rearrangement):

$$I_M^{\beta} = \frac{\alpha q_M + q_E}{\beta q_M + q_E} \tag{23}$$

Finally, substitution of eq 23 into eq 22 yields the measured excimer-to-monomer ratio as a function of multimer concentration through a weighted average of α and β:

$$R = \frac{\sum_{i=1}^{n-1} i[\text{P-EP}_i]\alpha + \sum_{j=n}^{\infty} j[\text{P-EP}_j]\beta\dfrac{\alpha q_M + q_E}{\beta q_M + q_E}}{\sum_{i=1}^{n-1} i[\text{P-EP}_i] + \sum_{j=n}^{\infty} j[\text{P-EP}_j]\dfrac{\alpha q_M + q_E}{\beta q_M + q_E}} \tag{24}$$

From eqs 11 and 12, one can calculate $[\text{P-EP}_k]$ at any concentration with an estimated equilibrium constant by introducing:

$$c_{\alpha} = \sum_{k=1}^{n-1} k[\text{P-EP}_k] \quad \text{and} \quad c_{\beta} = c - c_{\alpha} \tag{25}$$

and $Q = q_E/q_M = 0.49/0.65$.[10] Equation 24 then becomes

$$R = \frac{\alpha c_{\alpha} + \beta\dfrac{\alpha + Q}{\beta + Q}(c - c_{\alpha})}{c_{\alpha} + \dfrac{\alpha + Q}{\beta + Q}(c - c_{\alpha})} \tag{26}$$

and one can fit the function $R(\alpha,\beta,K_0,n,c)$ to the measured excimer-to-monomer ratios. This means a fitting of four parameters. The number of parameters could be reduced if the excimer-to-monomer ratio is known at infinitely low concentration (α is known in that case). The other parameter, β, can be measured also with some limited accuracy [see Figure 6; $\beta = R$ at a sufficiently high concentration (0.09 g/L) where the aggregation reaches its fullest extent].

The parameter n must be a small integer. This means that the fitting can be done by using different values for n (2, 3, 4) and comparing the results. In essence, it is the elimination of n from the fitting procedure. Results of the fitting procedure are compiled in Table 5.

The equilibrium constants assessed (Table 5) allowed the calculation of aggregation numbers. They are presented in Figure 8 for all three cases (n = 2, 3, and 4) with their inaccuracy. Clearly, the equilibrium constant obtained from the case $n = 3$ predicts the aggregation number best when the maximum concentration used in the fitting is 0.093 g/L. The curves shown in Figure 7 yield similar equilibrium constants with different α and β values.

The obtained equilibrium constants permitted the evaluation of the Gibbs free energy of the aggregation (Table 5). Using the value of $K_0 = (1.3 \pm 0.4) \times 10^7$ L/mol and converting it into a mole-fraction-based equilibrium constant (K') gave $\Delta G° = -RT \ln K' = -RT \ln (K_0 d_{\text{hexane}}/M_{\text{hexane}}) = -44.9 \pm 0.8$ kJ/mol as the most probable value for the dimerization reaction of two polymer molecules where d_{hexane} and M_{hexane} are the density and molecular weight of hexane, respectively. It is obvious from Table 5 that the Gibbs free energies are obtained with reasonably low errors, in spite of the large inaccuracies of the equilibium constant. Taking into account all of the uncertainties of $\Delta G°$, one can conclude that the Gibbs free energy change of the polymer association for each step is $\Delta G° = -45 \pm 4$ kJ/mol.

Conclusion

Substantial insight has been gained into the concentration-dependent association of a maleic anhydride-grafted ethylene–propylene copolymer (containing 60 mol % of ethylene), EP(60/40), in hexane and in THF by analyzing the results obtained in static and dynamic light scattering, gel exclusion chromatographic, and absorption and emission spectroscopic measurements. In particular, EP(60/40) and its pyrene-labeled analogue, P-EP(60/40), have

Table 5. Assessment of Equilibrium Constants for the Association of P-EP(60/40)[a]

max c, g/L	α	β	K_0, L/mol	$-\Delta G°$, kJ/mol[b]
$n = 2$[c]				
0.20	0.205 ± 0.029	0.506 ± 0.007	$(3.2 \pm 1.3) \times 10^6$	41.4
0.093	0.174 ± 0.026	0.494 ± 0.005	$(4.7 \pm 1.5) \times 10^6$	42.4
0.069	0.163 ± 0.029	0.490 ± 0.005	$(5.3 \pm 1.8) \times 10^6$	42.7
$n = 3$[d]				
0.20	0.227 ± 0.027	0.505 ± 0.007	$(8.9 \pm 3.4) \times 10^6$	43.9
0.093	0.198 ± 0.025	0.493 ± 0.005	$(1.3 \pm 0.4) \times 10^7$	44.9
0.069	0.189 ± 0.027	0.490 ± 0.005	$(1.4 \pm 0.5) \times 10^7$	45.0
$n = 4$[e]				
0.20	0.233 ± 0.027	0.505 ± 0.007	$(1.8 \pm 0.6) \times 10^7$	45.7
0.093	0.205 ± 0.025	0.493 ± 0.005	$(3.5 \pm 0.8) \times 10^7$	46.5
0.069	0.195 ± 0.026	0.490 ± 0.005	$(2.8 \pm 0.9) \times 10^7$	46.7

[a] See Results and Discussion section for details and Figure 6 for α and β. [b] $\Delta G° = -RT \ln K' = -RT \ln(K_0 C_{hex})$ where C_{hex} is a constant to convert the equilibrium constant (K_0) to mole fraction base $C_{hex} = d_{hexane}/M_{hexane}$. [c] β is reached in the dimer. [d] β is reached in the trimer. [e] β is reached in the tetramer.

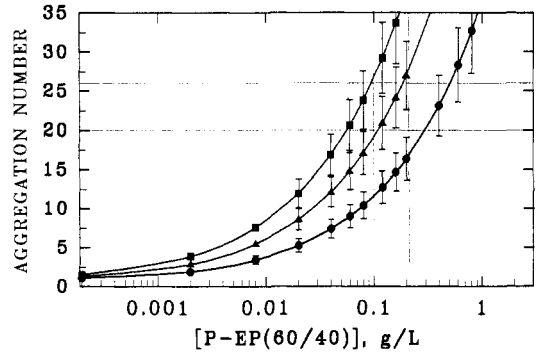

Figure 8. Mass-averaged aggregation numbers and their inaccuracies calculated from the different equilibrium constants as a function of P-EP(60/40) concentration. The β excimer–monomer ratio is reached by the dimer, $K_0 = 4.7 \times 10^6$ L mol^{-1} (●), trimer, $K_0 = 1.3 \times 10^7$ L mol^{-1} (▲), and tetramer, $K_0 = 2.5 \times 10^7$ L mol^{-1} (■). The cross section of the horizontal and vertical line pairs indicates the aggregation number at the corresponding concentration range obtained from steady-state light scattering.

been found to have relatively low molecular weight and to undergo ground-state association in hexane (but not in THF) in the 0.001–0.3 g/L concentration range.

Treatment of excimer-to-monomer ratios, determined as a function of the concentration of P-EP(60/40), has been particularly fruitful. It allowed the assessment of the equilibrium constant of association, aggregation numbers, and the Gibbs free energy of association ($\Delta G°$) of the copolymer in hexane. The absolute value of $\Delta G°$ was found to be rather high considering that only secondary interactions between individual molecules is believed to be responsible for the aggregation of P-EP(60/40). Based on $\Delta G°$, it is unreasonable to assume that polar interactions of the succinimide groups alone are the driving force for such an effective association. Formation of small ordered domains (or "crystallites") due to sufficiently long ethylene sequences which bridge different molecules (Figure 9), as suggested elsewhere,[5] may well contribute to the observed $\Delta G° = -45 \pm 4$ kJ/mol. Since hexane is a better solvent than THF for EP(60/40), one might expect a stronger association in the latter solvent than in the former. The opposite case has been found, however. The combined effect of dipole–dipole interaction between the succinimide groups in hexane (Figure 9) and the "crystallite" formation may well explain this behavior. In hexane, the interaction of polar groups and the formation of pyrene ground-state complexes may bring different molecules into close contact for a period which is sufficiently long enough to nucleate

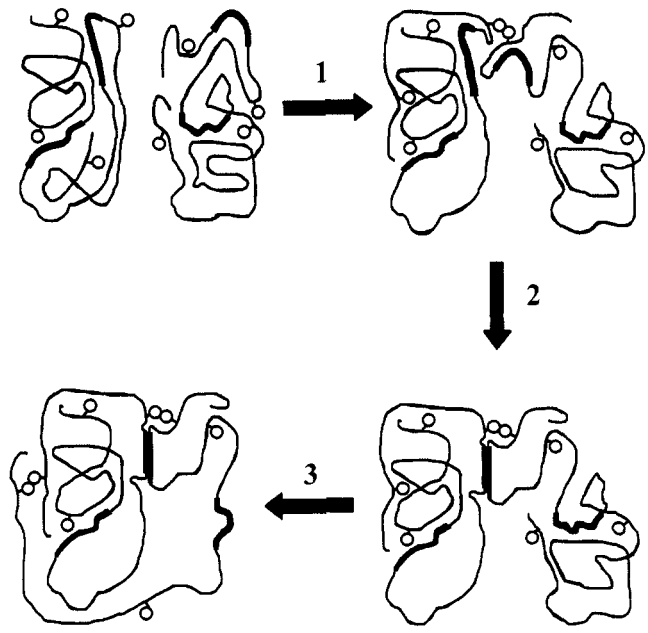

Figure 9. Proposed model of P-EP(60/40) association at high dilution. Step 1: The higher molecular weight components of P-EP(60/40) with several labels (denoted by circles) and long segments of ethylene sequences (represented by thick lines) are bridged by the formation of a ground-state pyrene complex due to the strong dipole–dipole interaction of the succinimide groups in hexane. Step 2: The long ethylene sequences (held close to each other by the pyrene complex) interact for a sufficiently long time to form an ordered domain with the involvement of chain segments from both molecules. Step 3: Additional linkages render the association highly favorable.

the growth of ordered domains. In THF, however, the nucleation process is prevented by solvent shielding of the polar interactions between the polymer chains.

Another interesting phenomenon has been revealed in the investigation of P-EP(60/40) association. The model which was used for the estimation of the equilibrium constant, with the assumption of identical molecules in the system, predicts a continuously increasing weight-averaged aggregation number with increasing P-EP(60/40) concentration. Conversely, the aggregation number has not been found to change appreciably, by static and dynamic light scattering, in the 0.1–3.0 g/L of EP(60/40) concentration range (Figure 1). This discrepancy is likely to originate in the polydispersity of the sample used. The average driving force for the aggregation of higher molecular weight polymers is greater than that for their lower molecular weight counterparts, due to the increased probability of finding polar groups and long ethylene sequences on them. For these molecules, association can be efficient, even in the most dilute solutions, leading to a system of large aggregates in a solution which contains lower molecular weight P-EP(60/40) components. Upon increasing the concentration, the previously formed aggregates, acting as cores, would be covered with smaller P-EP(60/40). This process would initiate less and less increase in the mass of the aggregates with increasing P-EP(60/40) concentration and would lead to practically constant hydrodynamic diameters and mass-averaged apparent molecular weights (see Figure 10). In a different process, small aggregates of relatively low molecular weight copolymers may also appear at higher P-EP(60/40) concentrations. The coverage of the core (formed by the association of higher molecular weight copolymers) by a shell of small molecules with decreased capacity of aggregation would then prevent further association and would keep the solution stable. Increasing the concentra-

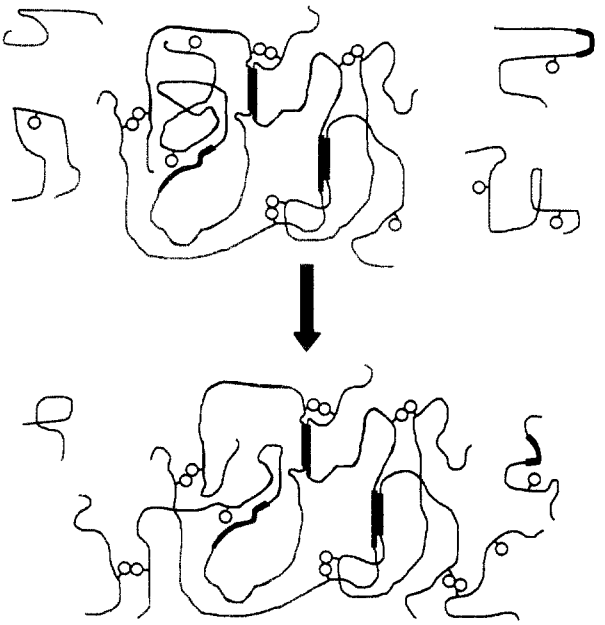

Figure 10. Proposed model of EP(60/40) association at higher concentrations. An aggregate of three large molecules is shown with other small molecules. Due to the increased concentration, the smaller molecules of P-EP(60/40) can interact with other solutes more effectively. They can attach to the previously formed aggregates (which act as loose cores) and can also form smaller aggregates (not shown). Upon attachment to the large aggregate, the bridging points are blocked, a loose shell of molecules without additional bridging groups is formed, and further growth is prevented. Circles represent the polar groups, and thick lines represent the long ethylene sequences.

tion of P-EP(60/40) to a degree at which coil overlap is inevitable would result in the formation of transient networks which would manifest in a sharp increase of the apparent hydrodynamic diameter. This, in fact, was the observed experimental result in hexane solutions when the EP(60/40) concentration was greater than about 3 g/L (Figure 1).

The rich variety of complex behavior of ethylene–propylene copolymers is, perhaps, the most obvious conclusion of the present work. Concentration-dependent aggregation of EP(60/40) is quite different in hexane and THF; it is also different from that observed for its higher molecular weight counterpart.[4]

Acknowledgment. Support of this work by grants from Texaco, Inc. (Beacon, NY), and the National Science Foundation is gratefully acknowledged.

References and Notes

(1) Syracuse University.
(2) Texaco R&D Department.
(3) Strate, G. V.; Struglinski, M. J. In *Polymers as Rheology Modifiers*; Schulz, D. N., Glass, J. E., Eds.; ACS Symposium Series 466; American Chemical Society: Washington, DC, 1991; p 256.
(4) Rubin, I. D.; Sen, A. In *Polymers as Rheology Modifiers*; Schultz, D. N., Glass, J. E., Eds.; ACS Symposium Series 466; American Chemical Society: Washington, DC, 1991; p 273.
(5) Sen, A.; Rubin, I. D. *Macromolecules* **1990**, *23*, 2519.
(6) Kucks, M. J.; Ou-Yang, H. D.; Rubin, I. D. *Macromolecules* **1993**, *26*, 3846.
(7) Jao, T.-C.; Mishra, M. K.; Rubin, I. D. *Macromol. Rep.* **1992**, *A29*, 283.
(8) Jao, T.-C.; Mishra, M. K.; Rubin, I. D.; Duhamel, J.; Winnik, M. A. *J. Polym. Sci.*, in press.
(9) Inoue, K.; Watanabe, H. *ASLE Trans.* **1982**, *26*, 189.
(10) Németh, S.; Jao, T.-C.; Fendler, J. H. *J. Photochem. Photobiol.* **1994**, *78*, 229.
(11) Brown, J. C.; Pusey, P. N.; Dietz, R. *Chem. Phys.* **1975**, *62*, 1136.
(12) Knapstad, B.; Skjølsvik, P. A.; Øye, H. A. *J. Chem. Eng. Data* **1989**, *34*, 37.
(13) Riddick, J. A.; Bunger, W. B.; Sakano, T. K. *Organic Solvents: Techniques of Chemistry Volume II*, 4th ed.; John Wiley & Sons: New York, 1986; p 310.
(14) Approximates the polymer coils as cubes with an edge of 40 nm gives a particle volume of 6.4×10^{-20} L which corresponds to a maximum number of 1.6×10^{19}, not overlapping EP coils in a 1-L volume. Therefore, the lower limit of the maximum concentration at which individual coils can exist is 2.6×10^{-5} mol/L. Multiplication by the number-averaged molecular weight gives 0.4 g/L, and it is the lower limit since the number-averaged molecular weight is smaller than the one obtained from light scattering.
(15) Benoit, H.; Froleich, D. In *Light Scattering from Polymer Solutions*; Huglin, M. B., Ed.; Academic Press: London and New York, 1972; p 467.
(16) Huglin, M. B.; Elias, H.-G. In *Light Scattering from Polymer Solutions*; Huglin, M. B., Ed.; Academic Press: London and New York, 1972; p 262.
(17) Evans, J. M. In *Light Scattering from Polymer Solutions*; Huglin, M. B., Ed.; Academic Press: London and New York, 1972; p 89.
(18) Winnik, F. M. *Chem. Rev.* **1993**, *93*, 587.
(19) Winnik, M. A. *Acc. Chem. Res.* **1985**, *18*, 73.
(20) Lix, X.-B.; Winnik, M. A.; Guillet, J. E. *Macromolecules* **1983**, *16*, 992.
(21) Ito, K.; Guillet, J. E. *Macromolecules* **1979**, *12*, 1163.
(22) Winnik, F. M.; Winnik, M. A.; Tazuke, S.; Ober, C. K. *Macromolecules* **1987**, *20*, 38.
(23) Elias, H.-G. In *Light Scattering from Polymer Solutions*; Huglin, M. B., Ed.; Academic Press: London and New York, 1972; p 397.
(24) Elias, H.-G. *Macromolecules 1*, 2nd ed.; Plenum Press: New York and London, 1984; p 226.
(25) Birks, J. B. *Photophysics of Aromatic Molecules*; John Wiley & Sons: New York, 1971.